

# SINGLE AXIS POINTING BY MEANS OF TWO REACTION WHEELS

**Alessandro Zavoli<sup>(1)</sup>, Fabrizio Giulietti<sup>(2)</sup>, Giulio Avanzini<sup>(3)</sup>, and Guido De Matteis<sup>(4)</sup>**

<sup>(1)</sup>*'Sapienza' Università di Roma, Via Eudossiana 18, Rome, Italy 00184, (+39) 064458 5210, alessandro.zavoli@uniroma1.it*

<sup>(2)</sup>*Università di Bologna, Via Fontanelle 40, Forlì, Italy 47121, (+39) 0543 374424, fabrizio.giulietti@unibo.it*

<sup>(3)</sup>*Università del Salento, Campus Ecotekne, Lecce, Italy 73100, (+39) 0832297798, giulio.avanzini@unisalento.it*

<sup>(4)</sup>*'Sapienza' Università di Roma, Rome, Italy 00184, (+39) 064458 5210, guido.dematteis@uniroma1.it*

**Abstract:** *The paper deals with attitude dynamics of an underactuated spacecraft, proposing a technique for aiming a body-fixed axis (e.g. sensor, antenna, nozzle, etc.) arbitrarily close to a prescribed direction in space by means of two reaction wheels only, when the total angular momentum of the spacecraft is zero. The technique is based on a simple kinematic planning scheme, where an eigenaxis rotation is performed around an admissible rotation axis, that is, an axis that lies on the plane of the two active reaction wheels. Proof of almost global stability is provided, together with a detailed discussion of a few theoretical shortcomings. The latter can be circumvented in the numerical implementation of the control law, that remains simple and computationally efficient. Numerical simulations of single-axis pointing maneuvers for a reference spacecraft prove the practical viability and validity of the approach. The effect of non-ideal conditions, such as a small residual angular momentum, command torque saturation and off-diagonal terms in the inertia tensor, are also investigated.*

**Keywords:** *Attitude control, Underactuated control, Reaction wheel failure.*

## 1. Introduction

The paper proposes a novel approach for single-axis pointing by using only two reaction wheels (RW), derived on the basis of a simple yet effective wheel rate command. This maneuver technique can be used for aiming the line-of-sight of a sensor, a nozzle or an antenna towards a target direction, or solar panels towards the Sun, after failure of one wheel for a non-redundant control system hardware or in the case of multiple failures for redundant systems. Examples of this kind of situation are the Far Ultraviolet Spectroscopic Explorer (FUSE) and Kepler space telescope, that both suffered from failures that left only two wheels available for maneuvers. Failure of mechanical actuators is also expected to potentially affect low-budget space missions based on small-size low-cost spacecraft (nano-, pico-, and cube-sat families).

The control approach here proposed, derived from the kinematic planning scheme of Ref. [1], represents its practical, dynamic implementation, under the assumptions of zero overall angular momentum and a diagonal inertia tensor. The effects of a non-zero residual angular momentum and control axes not aligned with the principal axes of inertia will also be investigated at the end of the paper, highlighting limitations on pointing precision and convergence performance. The possibility of pointing a body-fixed axis towards and arbitrary direction represents a significant contribution,

inasmuch as it may allow a failed spacecraft to perform, at least partially, its operational tasks. The limited computational effort for the control law makes it a practical solution also in the case of small-size satellites, where computational budget is severely limited by the available CPU processing capabilities.

The problem of spacecraft control by means of two attitude effectors only is a relevant topic in the literature dealing with satellite attitude control. Among many others, Tsiotras and Longuski [2] present a methodology for constructing feedback control laws for the attitude stabilization about the symmetry axis. Kim & Kim [3] also consider the problem of spin stabilization of a spacecraft about a specified inertial axis using two reaction wheels. They exploit the  $z$ - $w$  parametrization introduced by Tsiotras [4] to derive a feedback control law that globally and asymptotically stabilizes the spacecraft on a revolving motion along a specified inertial axis.

A time-variant discontinuous singular controller approach is proposed by Horri for the 3-axis attitude stabilization of a zero total angular momentum satellite, based on a Rodriguez parametrization of the attitude [5] or on a quaternion attitude parametrization [6]. Yoon and Tsiotras [7] consider a spacecraft equipped with a single VSCMG. They illustrate an LQR control law to locally stabilize the spacecraft angular velocity, while also controlling the direction of a given spacecraft body-axis in the inertial space. A multi-stage control law is also suggested to attain the same goal in the large.

In Ref. [1], Avanzini and Giulietti propose a kinematic planning scheme for eigenaxis rotations that allows for aiming a body-fixed axis  $\hat{\sigma}$  towards a prescribed direction  $\hat{\tau}$ , in the presence of constraints on the admissible rotation axis. This constraint is representative of a condition of underactuation for the attitude control system, when there is a direction  $\hat{\mathbf{b}}$  around which a control torque component is not available. This means that control torque is constrained on a plane perpendicular to the torqueless direction. This technique has been recently extended in order to determine a sequence of feasible rotations with minimum total angular path, to be applied when the axis  $\hat{\sigma}$  is also required to stay away from inadmissible directions, such as bright radiation sources that may harm sensor hardware [8].

The kinematic planning schemes of Refs. [1] and [8] identify a (sequence of) admissible rotation(s), represented in terms of eigenaxis  $\hat{\mathbf{g}}_{\Gamma}$ , perpendicular to  $\hat{\mathbf{b}}$ , and rotation amplitude  $\hat{\alpha}$ , that allows for driving  $\hat{\sigma}$  towards a prescribed direction  $\hat{\tau}$ . The approach proposed in Refs. [1] and [8] is applied as a maneuver planning scheme in the framework of magnetic control, where magnetic torquers are used as attitude effectors and the torqueless direction  $\hat{\mathbf{b}}$  is represented by the geomagnetic field, being thus prescribed in the orbit frame. But, as underlined in [1], the same planning scheme can also be adopted when the torqueless direction  $\hat{\mathbf{b}}$  is prescribed in the body frame.

In the present paper, the kinematic planning scheme of Ref. [1] is turned into a control logic and it is applied to the case of a spacecraft equipped with only two operational reaction wheels. As outlined above, such a situation is representative of failure conditions for non-redundant control hardware of multiple failure in a redundant system. Thanks to simple angular momentum balance considerations, it is possible to derive a wheel rate command that causes the spacecraft to rotate around the admissible rotation axis,  $\hat{\mathbf{g}}_{\Gamma}$ , lying on the plane identified by the two RW axes, thus directly implementing the kinematic planning scheme at a dynamic level. This is obtained by

defining a desired angular velocity command around the admissible rotation axis  $\hat{\mathbf{g}}_\Gamma$ , the magnitude of which is proportional to the amplitude  $\hat{\alpha}$  of the admissible rotation.

A candidate Lyapunov function is then defined, which features two terms, one proportional to the remaining angular travel towards  $\hat{\tau}$ , one to the error of the current angular speed with respect to the desired angular velocity. A reaction wheel command torque is derived, which guarantees that the time derivative  $\dot{V}$  of the candidate Lyapunov function is strictly negative, thus enforcing an asymptotic convergence of  $\hat{\sigma}$  towards the desired direction  $\hat{\tau}$  for almost any initial condition.

Convergence is straightforward, once the direction of the admissible rotation axis  $\hat{\mathbf{g}}_\Gamma$  is available. As a minor drawback, there are some situations in which the definition of this axis can become critical, that is when  $\hat{\sigma}$  and  $\hat{\tau}$  are exactly aligned (that is, the desired alignment is obtained), and when the alignment error  $\varepsilon = \hat{\tau} - \hat{\sigma}$  is parallel to the torqueless direction  $\hat{\mathbf{b}}$ . The first case is not critical, provided also that the magnitude of the angular velocity command drops to zero when the desired alignment is achieved. The second case will deserve an ad hoc discussion.

In the next Section, after some preliminary considerations, the derivation of the control law for the zero-angular momentum case is provided, with a proof of stability and a discussion of the critical situation highlighted above. In Section III, convergence towards the prescribed axis alignment is analyzed by means of numerical simulation, also in the case of a non-zero residual angular momentum and for a non-diagonal inertia tensor. A Section of concluding remarks ends the paper.

## 2. Problem Statement and solution

### 2.1. Outline of the kinematic planning scheme

The approach here proposed allows for a computationally inexpensive control technique that directly stems from the kinematic planning scheme of [1], representing its practical, dynamic implementation, under the assumption of zero overall angular momentum. An ideal admissible rotation eigenaxis  $\hat{\mathbf{g}}_\Gamma$  is identified, which allows for aiming a body-fixed axis  $\hat{\sigma}$  towards a prescribed direction  $\hat{\tau}$ , when the admissible rotation axis is constrained to lie on a plane perpendicular to the torqueless direction  $\hat{\mathbf{b}}$ .

The body-fixed axis  $\hat{\sigma}$  can be rotated onto its desired position  $\hat{\tau}$  by means of an eigenaxis rotation of amplitude  $\hat{\alpha}$  around one of the axis

$$\hat{\mathbf{g}} = \hat{\mathbf{e}}_m \cos \beta + \hat{\mathbf{e}}_M \sin \beta \quad (1)$$

where  $\hat{\mathbf{e}}_m = (\hat{\sigma} \times \hat{\tau}) / \|\hat{\sigma} \times \hat{\tau}\|$  is perpendicular to the plane that contains  $\hat{\sigma}$  and  $\hat{\tau}$ ,  $\hat{\mathbf{e}}_M = (\hat{\sigma} + \hat{\tau}) / \|\hat{\sigma} + \hat{\tau}\|$  is the bisector between  $\hat{\sigma}$  and  $\hat{\tau}$ , and  $\beta$  is the angle between  $\hat{\mathbf{g}}$  and  $\hat{\mathbf{e}}_m$ . For  $\beta = 0$ , the desired alignment of  $\hat{\sigma}$  over  $\hat{\tau}$  is obtained by means of the minimum angular path,  $\alpha$ , that is, the angle between  $\hat{\sigma}$  and  $\hat{\tau}$  at the initial time.

The admissible rotation axis was then identified in [1] by choosing the angle  $\beta$  that provides the unit vector  $\hat{\mathbf{g}}_\Gamma$  perpendicular to  $\hat{\mathbf{b}}$ , that is, the eigenaxis  $\hat{\mathbf{g}}_\Gamma$  is chosen at the intersection of the planes  $\Gamma$  and  $\Sigma$ , where  $\Gamma$  is perpendicular to  $\hat{\mathbf{b}}$  (identified in the present application by the plane that contains

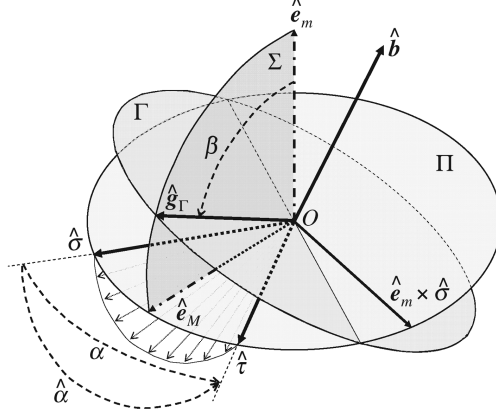


**Figure 1. Kinematic planning scheme (from [1]).**

the spin axis of the two active RW's), and  $\Sigma$ , which contains all the axes  $\hat{\mathbf{g}}$  that allow for performing the required alignment of  $\hat{\boldsymbol{\sigma}}$  over  $\hat{\boldsymbol{\tau}}$ , that is the plane identified by  $\hat{\mathbf{e}}_m$  and  $\hat{\mathbf{e}}_M$  (see Fig. 1). In the derivation of the control law, it is more convenient to express the admissible eigenaxis  $\hat{\mathbf{g}}_\Gamma$  in the form

$$\hat{\mathbf{g}}_\Gamma = \frac{(\hat{\boldsymbol{\tau}} - \hat{\boldsymbol{\sigma}}) \times \hat{\mathbf{b}}}{\|(\hat{\boldsymbol{\tau}} - \hat{\boldsymbol{\sigma}}) \times \hat{\mathbf{b}}\|} \quad (2)$$

where the error vector  $\boldsymbol{\varepsilon} = \hat{\boldsymbol{\tau}} - \hat{\boldsymbol{\sigma}}$  is perpendicular to the plane  $\Sigma$ , whereas the underactuated direction  $\hat{\mathbf{b}}$  is normal to the plane  $\Gamma$  that contains the admissible rotation axes.

The amplitude of the rotation  $\hat{\alpha}$  can be analytically determined (see [1] for details), and it depends on  $\beta$ , growing from its minimum value,  $\hat{\alpha} = \alpha$  for  $\beta = 0$  and  $\hat{\mathbf{g}} = \hat{\mathbf{e}}_m$ , up to  $\pi$  rad, when  $\beta = \pi/2$  and  $\hat{\mathbf{g}} \equiv \hat{\mathbf{e}}_M$ . Also this result was revisited for the derivation of the control law discussed in this paper. Thanks to spherical trigonometry considerations (omitted here for the sake of conciseness) it is possible to prove that

$$\sin(\hat{\alpha}/2) = \frac{\sin(\alpha/2)}{[\sin^2(\alpha/2) \sin^2 \beta + \cos^2 \beta]^{1/2}} \quad (3)$$

The idea at the basis of the present paper is to derive an angular rate command for the available wheels that results into a rotation of the spacecraft (almost exactly) around the admissible axis  $\hat{\mathbf{g}}_\Gamma$ . The desired angular rate achieves the form  $\boldsymbol{\omega}_d = \omega_d \hat{\mathbf{g}}_\Gamma$ , where the magnitude of the rate command,  $\omega_d$ , is proportional to the required angular travel  $\hat{\alpha}$  around  $\hat{\mathbf{g}}_\Gamma$ , that provides the required single axis pointing (that is,  $\hat{\boldsymbol{\sigma}}$  parallel to  $\hat{\boldsymbol{\tau}}$ ). In the ideal case, one assumes that a perfect detumbling and/or wheel desaturation of the spacecraft was performed prior to the pointing maneuver, such that the total angular momentum of the spacecraft is zero.

## 2.2. Equations of motion

A satellite platform equipped with three identical reaction wheels is considered. Spacecraft dynamics, expressed in terms of total angular momentum with respect a set of body-fixed principal axes of

inertia,  $\mathbb{F}_B = \{P, \hat{\mathbf{e}}_1, \hat{\mathbf{e}}_2, \hat{\mathbf{e}}_3\}$  centered in the spacecraft center of mass P, is described by the following equations:

$$\begin{aligned}\dot{\boldsymbol{\omega}} &= \mathbf{J}^{-1} [-\boldsymbol{\omega} \times (\mathbf{J}\boldsymbol{\omega} + \mathbf{h}_w) - \dot{\mathbf{h}}_w] \\ \dot{h}_{w,i} &= J_w \dot{\Omega}_i = g_{em,i} - J_w \dot{\boldsymbol{\omega}}^T \hat{\mathbf{a}}_i, \quad i = 1, 2, 3\end{aligned}\quad (4)$$

where  $\boldsymbol{\omega} = (\omega_1, \omega_2, \omega_3)^T$  is the absolute angular velocity vector,  $h_{w,i} = J_w \Omega_i$  is the relative angular momentum vector of the  $i$ -th reaction wheel that spins at a relative angular rate  $\Omega_i$  around the spin axis  $\hat{\mathbf{a}}_i$ , under the control of the electrical motor torque  $g_{em,i}$ , and  $\mathbf{J}$  is the spacecraft inertia matrix. The vector  $\mathbf{h}_w = \sum_{i=1}^3 J_w \Omega_i \hat{\mathbf{a}}_i$  is the total internal angular momentum.

It will be assumed that  $\hat{\mathbf{e}}_i$ ,  $i = 1, 2, 3$  are principal axes of inertia, the inertia tensor becomes diagonal,  $\mathbf{J} = \text{diag}(J_1, J_2, J_3)$  and that the spin axes of the wheels are parallel to them, that is,  $\hat{\mathbf{a}}_i \equiv \hat{\mathbf{e}}_i$ ,  $i = 1, 2, 3$ . Without loss of generality, one can also assume that the underactuated axis is  $\hat{\mathbf{b}} = \hat{\mathbf{e}}_3$ . As a consequence, only two reaction wheels are available, with spin axes parallel to the  $\hat{\mathbf{e}}_1$  and  $\hat{\mathbf{e}}_2$  body axes.

Under the assumption of zero total angular momentum, and neglecting external torques,  $\mathbf{h}$  is constantly zero; a vector  $\mathbf{u} = (u_1, u_2, u_3)^T$  of virtual controls  $u_i = -(T_{em,i} - J_w \dot{\boldsymbol{\omega}}^T \hat{\mathbf{a}}_i)$  can be introduced, so that Eq.s (4) and (5) reduces to

$$\mathbf{J}\dot{\boldsymbol{\omega}} = \mathbf{u} \quad (6)$$

$$\dot{\mathbf{h}}_w = -\mathbf{u} \quad (7)$$

Moreover, in the absence of an active reaction wheel spinning around  $\hat{\mathbf{e}}_3$ , the third component of the angular velocity vector  $\omega_3$  remains identically zero throughout the maneuver.

### 2.3. Command law and proof of stability

An asymptotical convergence to the desired single-axis pointing condition can be obtained if a stable first-order dynamics in the form

$$\dot{\hat{\alpha}} + k_\alpha \hat{\alpha} = 0 \quad (8)$$

is enforced to the rotation angle  $\hat{\alpha}$  about the unit vector  $\hat{\mathbf{g}}_\Gamma$ . It is possible to express the time derivative of  $\hat{\alpha}$  in the form

$$\dot{\hat{\alpha}} = \boldsymbol{\omega}^T \boldsymbol{\Psi}, \quad (9)$$

where

$$\boldsymbol{\Psi} = \frac{(\hat{\boldsymbol{\tau}} \times \hat{\boldsymbol{\sigma}}) + 2(1 - \cos \hat{\alpha})(\hat{\mathbf{g}}_\Gamma \cdot \hat{\boldsymbol{\sigma}}) \{ [\hat{\mathbf{g}}_\Gamma \times (\hat{\boldsymbol{\sigma}} \times \hat{\mathbf{g}}_\Gamma)] (\hat{\mathbf{b}} \cdot \hat{\boldsymbol{\tau}}) - [(\hat{\boldsymbol{\tau}} \times \hat{\mathbf{g}}_\Gamma) \cdot (\hat{\boldsymbol{\sigma}} \times \hat{\mathbf{g}}_\Gamma)] \hat{\mathbf{b}} \}}{\sin \hat{\alpha} [1 - (\hat{\mathbf{g}}_\Gamma \cdot \hat{\boldsymbol{\sigma}})^2]} \boldsymbol{\varepsilon} \times \hat{\mathbf{b}} \quad (10)$$

with  $\boldsymbol{\varepsilon} = \hat{\boldsymbol{\tau}} - \hat{\boldsymbol{\sigma}}$  (the derivation of Eq.s (10) is provided with full details in Appendix 1). An asymptotically stable dynamics for  $\hat{\alpha}$  is obtained if a desired angular speed in the form

$$\boldsymbol{\omega}_d = - [k_\alpha \hat{\alpha} / (\hat{\mathbf{g}}_\Gamma^T \boldsymbol{\Psi})] \hat{\mathbf{g}}_\Gamma \quad (11)$$

is tracked. Equation (11) can be further simplified noting that  $\hat{\mathbf{g}}_\Gamma^T \Psi = 1$  (proof is given in Appendix 2), hence

$$\boldsymbol{\omega}_d = -k_\alpha \hat{\alpha} \hat{\mathbf{g}}_\Gamma \quad (12)$$

Noting that  $\boldsymbol{\omega}_3$  and  $\boldsymbol{\omega}_{d,3}$  are both zero (the former because of conservation of angular momentum, and the latter from its definition that requires that  $\boldsymbol{\omega}_d$  lies on the plane of admissible rotations, normal to  $\hat{\mathbf{b}} \equiv \hat{\mathbf{e}}_3$ ), the third component of the vector  $\Psi$  (which in general is not zero) becomes not relevant for the dynamics of  $\hat{\alpha}$ . At the same time, only the first two RW torque components are available. It is thus possible to define the following vector quantities,  $\boldsymbol{\omega}^* = (\boldsymbol{\omega}_1, \boldsymbol{\omega}_2)^T$ ,  $\boldsymbol{\omega}_d^* = (\boldsymbol{\omega}_{d,1}, \boldsymbol{\omega}_{d,2})^T$ ,  $\mathbf{u}^* = (u_1, u_2)^T$ , and  $\Psi^* = (\Psi_1, \Psi_2)^T$ .

In order to find a command  $\mathbf{u}^*$  for the operational RW's, which implements the single-axis pointing strategy with asymptotic convergence towards the desired inertially-fixed direction  $\hat{\boldsymbol{\tau}}$ , a strictly positive candidate Lyapunov function is then introduced,

$$V = \frac{1}{2} \hat{\alpha}^2 + \frac{1}{2} \mathbf{z}^{*T} \mathbf{J}^* \mathbf{z}^* \quad (13)$$

where  $\mathbf{z} = \boldsymbol{\omega}_d - \boldsymbol{\omega}$ , and  $\mathbf{z}^* = (z_1, z_2)^T$  is the error on the first and second components of the angular velocity, and  $\mathbf{J}^* = \text{diag}(J_1, J_2)$  is a reduced-order inertia matrix. By taking the time derivative of Eq. (13) one gets

$$\dot{V} = \hat{\alpha} \dot{\hat{\alpha}} + \mathbf{z}^{*T} \mathbf{J}^* \dot{\mathbf{z}}^* \quad (14)$$

After taking into account Eq. (9), and recalling that  $\boldsymbol{\omega} = \boldsymbol{\omega}_d - \mathbf{z}$ ,  $\dot{V}$  achieves the form

$$\dot{V} = -k_\alpha \hat{\alpha}^2 - \mathbf{z}^T \Psi \dot{\hat{\alpha}} + \mathbf{z}^{*T} (\mathbf{J}^* \dot{\boldsymbol{\omega}}_d^* - \mathbf{u}^*) \quad (15)$$

By noting that  $\mathbf{z}^T \Psi = \mathbf{z}^{*T} \Psi^*$ , one can rewrite  $\dot{V}$  as

$$\dot{V} = -k_\alpha \hat{\alpha}^2 - \mathbf{z}^{*T} (\Psi^* \dot{\hat{\alpha}} - \mathbf{J}^* \dot{\boldsymbol{\omega}}_d^* + \mathbf{u}^*) \quad (16)$$

The first term is clearly negative definite, for any value of  $\hat{\alpha}$  and  $k_\alpha > 0$ . If one selects the control  $\mathbf{u}^*$ , such that

$$\mathbf{z}^{*T} (\Psi^* \dot{\hat{\alpha}} - \mathbf{J}^* \dot{\boldsymbol{\omega}}_d^* + \mathbf{u}^*) = \mathbf{z}^{*T} \mathbf{C} \mathbf{z}^* > 0, \quad (17)$$

where  $\mathbf{C} \in \mathbb{R}^2$  is any positive definite symmetric matrix,  $\dot{V}$  becomes strictly negative and the desired pointing of  $\hat{\boldsymbol{\sigma}}$  is asymptotically achieved. This is obtained by letting

$$\mathbf{u}^* = \mathbf{C} \mathbf{z}^* - \Psi^* \dot{\hat{\alpha}} + \mathbf{J}^* \dot{\boldsymbol{\omega}}_d^* \quad (18)$$

## 2.4. Practical implementation

The implementation of Eq. (18) as the command law requires the determination of  $\dot{\boldsymbol{\omega}}_d$  during the maneuver. It is possible to derive an analytical expressions for  $\dot{\boldsymbol{\omega}}_d$  in terms of  $\dot{\hat{\alpha}}$  and  $\dot{\hat{\mathbf{g}}}_\Gamma$ , which becomes an undetermined form for  $\alpha \rightarrow 0$ . It is possible to prove that the limit remains finite, nonetheless computational issues are present in the numerical evaluation of this term for a practical implementation in a computer finite algebra. Moreover, the computational burden is increased by the complexity of the expressions, which feature several trigonometric terms.

As a consequence, it is easier and computationally more efficient to numerically evaluate  $\dot{\omega}_d$  by means of finite differences between the current value of  $\omega_d$  and its value at a previous time. This is particularly easy on a discrete time digital implementation and it circumvents all numerical issues with the determination of singular forms in the limit for vanishingly small values of  $\alpha$ .

In addition it is worth to remind that, since slow variations of  $\omega_d$  can be achieved by means of a proper choice of the control gains, the term containing  $\dot{\omega}_d$  is relatively small and thus it can be neglected in the definition of the control action. In this respect, in the next Section, together with the nominal command law given by Eq. (18), two more control laws are discussed: namely a simplified version

$$\mathbf{u}_S = \mathbf{C}\mathbf{z}^* - \Psi^* \hat{\alpha} \quad (19)$$

where the  $\dot{\omega}_d$  is dropped, and a minimum-complexity version, that is

$$\mathbf{u}_{MC} = \mathbf{C}\mathbf{z}^* = \mathbf{C}(\omega_d^* - \omega^*) \quad (20)$$

In this latter case, the control torque is simply required to track the desired value of the angular rates. Note that a proof of convergence becomes no longer available, when Eq. (19) or (20) are used. Simulations prove that convergence performance in both cases is still adequate (if not better).

As a final comment, note that in the proposed command law the angular rate command goes to zero as  $\hat{\sigma}$  approaches its desired position  $\hat{\tau}$ , thus slowing down the motion automatically. Command gains can be determined as a function of misalignment error  $\varepsilon$ , in order to speed up convergence when the error is large, by use of the maximum available wheel angular momentum.

### 3. Results

A spacecraft with moment of inertia  $\mathbf{J} = \text{diag}(40.45, 41.36, 42.09) \text{ kg m}^2$  was considered for demonstrating the viability of the approach. The two active reaction wheels have an identical moment of inertia,  $J_w = 0.0077 \text{ kg m}^2$ . Spacecraft data are taken from [5] in order to deal with a realistic set of parameters.

In the ideal case, the spacecraft and the reaction wheels are assumed to be at rest at the initial time ( $\omega_0 = 0$ ,  $\Omega_{i_0} = 0$ ), in order to satisfy the assumption of total angular momentum equal to zero during the maneuver. Without lack of generality, an inertially fixed target direction  $\hat{\tau}_I = (1, 0, 0)^T$  is assumed. Absence of any privileged inertial direction justifies this choice. Conversely, the position of the body-fixed axis  $\hat{\sigma}$  that needs to be aligned with  $\hat{\tau}$  has an influence on the response of the spacecraft, under the considered control law. Indicating with  $\lambda$  the elevation of  $\hat{\sigma}$  with respect to the plane of admissible rotations  $\Gamma$ , that is, the plane identified by the spin axes of the two active RW's ( $\hat{\mathbf{e}}_1$  and  $\hat{\mathbf{e}}_2$ , for the considered application), three cases are envisaged, namely: Case 1 for  $\lambda = 0$  (that is,  $\hat{\sigma}$  lies exactly on  $\Gamma$ ); Case 2 for  $0 < |\lambda| < \pi/2$  (that is,  $\hat{\sigma}$  lies outside of  $\Gamma$ ); and Case 3 for  $|\lambda| = 90 \text{ deg}$  (when  $\hat{\sigma}$  is parallel to the torqueless direction  $\hat{\mathbf{b}}$ , that is, the spin axis  $\hat{\mathbf{e}}_3$  of the failed reaction wheel). Note that, when  $\lambda = 0$ , the possibility of distributing the angular momentum over  $\Gamma$  between two wheels allows one to consider  $\hat{\sigma} \equiv \hat{\mathbf{e}}_i$ ,  $i = 1, 2$ , without loss of generality. In what follows,  $\hat{\sigma} \equiv \hat{\mathbf{e}}_1$  will be assumed for simulations testing the algorithm in Case 1 scenarios.

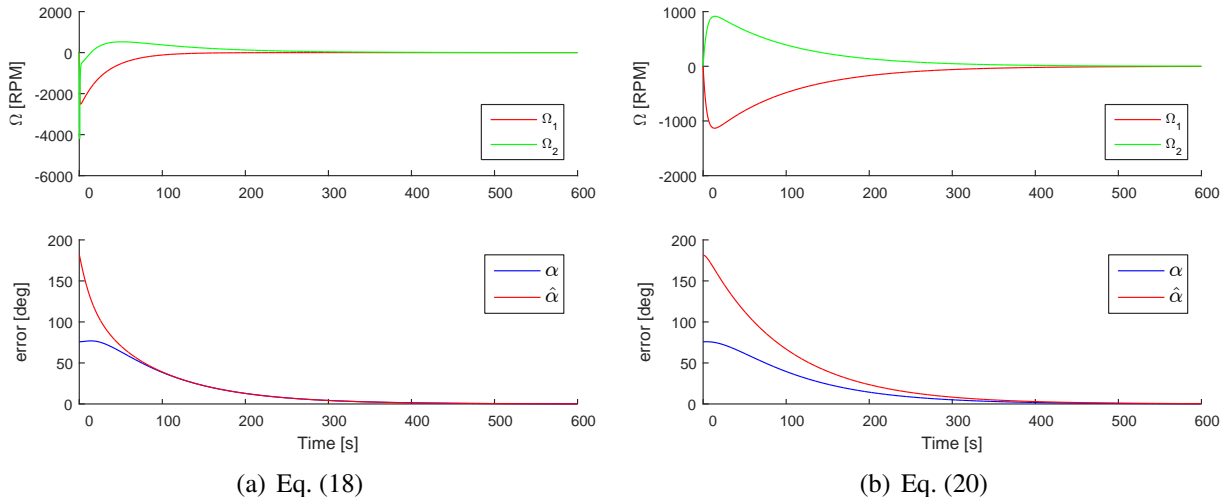


Figure 2. **Case 1 with  $\mathbf{h} = \mathbf{0}$ : wheel rates and pointing error for the nominal (a) and minimum-complexity (b) command laws.**

The results shown in the present section were obtained for control gains  $k_\omega = 100$  and  $k_\alpha = 0.001$ . These gains are not optimized, rather they were chosen with a trial-and-error procedure until a satisfactory convergence was obtained, without violating saturation constraints on maximum wheel rotation rate. All the three command laws proposed in the previous section, namely Eqs. (18), (19), and (20), were implemented for the ideal case, with zero total angular momentum, diagonal inertia tensor, and no saturation on RW command torque. In order to assess the command law in a more realistic scenario, some cases were also run in the presence of RW command torque saturation, non-diagonal inertia tensor and non-zero total angular momentum.

All the three command laws perform well in the ideal case for all the test-cases considered, that is, for an arbitrary direction of the axis  $\hat{\sigma}$  in the body frame. For  $\lambda = 0$  and a random initial attitude, described by the quaternion  $\mathbf{q}_{BI} = (0.7792, 0.1225, -0.1051, 0.6056)^T$ , the results reported in Fig. 2 are obtained using the complete and the minimum complexity command laws (Fig. 2(a) and (b), respectively). The behavior of the simplified law, where only the  $\dot{\omega}_d$  term is dropped, is almost identical to that of the complete law and it is not reported for the sake of conciseness.

From the comparison of the bottom plots in Figs. 2(a) and (b) it is apparent that the pointing error  $\alpha$  and the non-nominal rotation angle  $\hat{\alpha}$  share an almost identical behavior, with a convergence time in the same order of magnitude, only slightly above 500 s for the slower minimum complexity law. A more relevant difference is evident in the wheel rotation rate (and consequently in spacecraft angular speed components, not reported in the figures), visible in the top portion of the same figure, where  $\Omega_2$  has a different sign during the initial transient that accelerates the spacecraft around the admissible rotation axis  $\hat{\mathbf{g}}_T$ . This is due to the additional terms in the complete law, that are necessary to exactly cancel out the “fast terms” in spacecraft rotational dynamics. These terms are required in the proof of asymptotic stability, in order to obtain a strictly negative definite Lyapunov function (see Section 2), but they also result into more demanding RW command torques, with a faster initial transient and higher peaks in rotation rates during the first few seconds. As a matter of fact, the minimum complexity command law is simpler, computationally more efficient and it limits

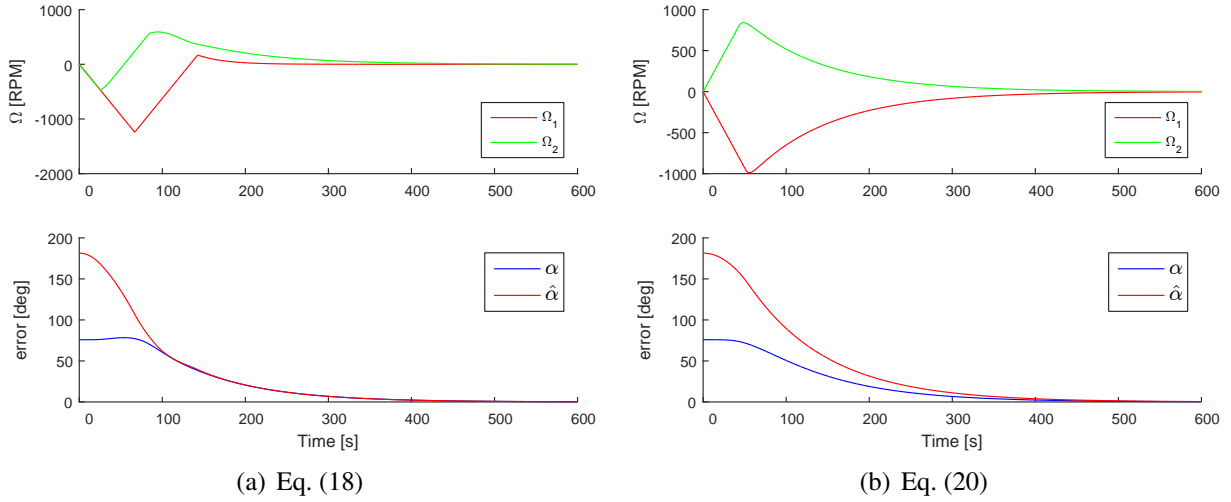


Figure 3. **Case 1 with  $h = 0$ : wheel rates and pointing error for the nominal (a) and minimum-complexity (b) command laws.**

the value of the torque commands at the beginning of the maneuver.

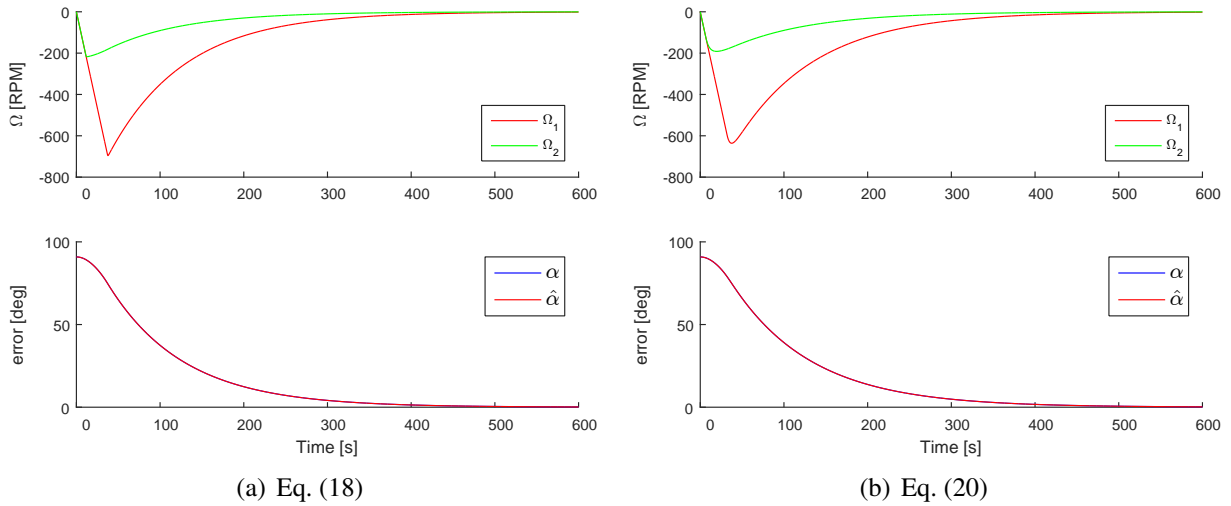


Figure 4. **Case 3 with  $h = 0$ : wheel rates and pointing error for the nominal (a) and minimum-complexity (b) command laws.**

Both laws are affected by saturation on the RW command torque in a similar way (Fig. 3(a) and (b)), where the initial acceleration transient becomes longer. Obviously, the effect of saturation is apparent on the behaviour of RW spin rates, which vary linearly during those time intervals when the command torque  $\mathbf{u}$  saturates. Nonetheless, the final convergence time to the desired alignment of  $\hat{\sigma}$  over  $\hat{\tau}$  is only marginally affected by the initial saturation of the command torque.

When a Case 3 scenario is dealt with, the behaviour of the complete and minimum complexity command laws becomes almost identical, clearly indicating that in this circumstance the additional terms required in the complete law for canceling the fast dynamics become less relevant, even in the presence of torque saturation, as shown in Fig. 4.

The misalignment of the command axes with respect to the principal axes of inertia has apparently no impact on the convergence characteristics of the command law. This situation was investigated by changing the nominal diagonal inertia tensor  $\mathbf{J}$  with a “full” inertia tensor  $\mathbf{J}_F = \mathbf{T}_m \mathbf{J} \mathbf{T}_m^T$ , where  $\mathbf{T}_m$  is a coordinate transformation matrix that expresses the misalignment of the control axes with respect to the frame of principal axes of inertia. For a 10 deg rotation around a random axis,  $\hat{\mathbf{a}} = (-0.4913, 0.8222, -0.2873)^T$ , one gets

$$\mathbf{J}_m = \begin{bmatrix} 40.4731 & -0.0801 & -0.1337 \\ -0.0801 & 42.0811 & 0.0536 \\ -0.1337 & 0.0536 & 41.3458 \end{bmatrix} \text{ kg m}^2 \quad (21)$$

For  $\lambda > 0$  (that is Cases 2 and 3), the perturbation of the alignment of the control axes has no consequences on the convergence to the desired alignment of  $\hat{\sigma}$  over  $\tau$ . Conversely, for  $\lambda = 0$ , the system converges steadily towards a solution with a small, yet non negligible, steady state error, that for the considered test cases, can become equal to 0.2 deg in terms of  $\alpha$ .

Finally, the effect of a small non-zero initial angular momentum stored in the RW’s is considered. This is a particularly relevant feature for small-size spacecraft equipped with magnetic actuators that, during the detumbling phase, dumps the angular momentum in excess, possibly close to zero, but never exactly canceling all the three components at the same time. As far as the single-axis pointing problem is dealt with, there is no apparent difficulty for the considered command law to aim exactly a body-fixed axis towards a desired direction, if the residual angular momentum is sufficiently small (in the order of 0.01 ÷ 0.1 Nms). For higher values of the angular momentum, some regions of the attitude space become not accessible when the spacecraft is at rest. Therefore, aligning an arbitrary (non-principal axes of inertia) body-axis  $\hat{\sigma}$  towards a given inertially-fixed direction may not be always possible. This is the subject of ongoing research

#### 4. Conclusions

The dynamic implementation of a kinematic planning strategy for single-axis pointing by means of two reaction wheels was demonstrated. An almost global stability to the desired alignment of a body-fixed axis towards an inertially fixed direction was given in ideal conditions of zero total angular momentum, no reaction wheel torque saturation and wheel spin axis aligned with the principal axes of inertia. The resulting command law features three terms: one required for generating an angular rate command that tracks the desired rotation around an admissible rotation axis (that is, a rotation axis that lies on the plane of the two active reaction wheels; a second one, related to the time-derivative of the angular rate command; and the third one, proportional to the angular travel required to perform the admissible rotation, in the direction of the vector that describes the evolution of this angle, as a function of the actual spacecraft angular speed. As a matter of fact, numerical simulation demonstrates that even simplified versions of the command law, where the second and the third terms are dropped, perform well also in non-ideal conditions, when a small residual angular momentum is dealt with, the inertia tensor features non-zero off-diagonal elements and saturation affects the maximum reaction wheel torque.

## Appendix 1

According to Rodrigues' rotation formula the unit vector  $\hat{\tau}$  can be seen as the rotation of  $\hat{\sigma}$  by an angle  $\hat{\alpha}$  about the axis  $\hat{\mathbf{g}}_\Gamma$

$$\hat{\tau} = \cos \hat{\alpha} \hat{\sigma} + \sin \hat{\alpha} (\hat{\mathbf{g}}_\Gamma \times \hat{\sigma}) + (1 - \cos \hat{\alpha}) (\hat{\mathbf{g}}_\Gamma \cdot \hat{\sigma}) \hat{\mathbf{g}}_\Gamma \quad (22)$$

After recalling that  $\hat{\tau} \cdot \hat{\sigma} = \cos \alpha$ , one has:

$$\cos \alpha = \cos \hat{\alpha} + (1 - \cos \hat{\alpha}) (\hat{\mathbf{g}}_\Gamma \cdot \hat{\sigma})^2 \quad (23)$$

By taking time derivative in the body-axis reference frame, one obtains

$$\dot{\hat{\alpha}} = \frac{\dot{\alpha} \sin \alpha + 2(1 - \cos \hat{\alpha}) (\hat{\mathbf{g}}_\Gamma \cdot \hat{\sigma}) (\dot{\hat{\mathbf{g}}}_\Gamma \cdot \hat{\sigma})}{\sin \hat{\alpha} (1 - (\hat{\mathbf{g}}_\Gamma \cdot \hat{\sigma})^2)} \quad (24)$$

where

$$\dot{\alpha} = -\hat{\mathbf{e}}_m \cdot \boldsymbol{\omega} \quad (25)$$

$$\dot{\hat{\mathbf{g}}}_\Gamma = \hat{\mathbf{g}}_\Gamma \times (\mathbf{a} \times \hat{\mathbf{g}}_\Gamma) \quad (26)$$

with

$$\mathbf{a} = (\dot{\boldsymbol{\varepsilon}} \times \hat{\mathbf{b}}) / \|\boldsymbol{\varepsilon} \times \hat{\mathbf{b}}\| \quad (27)$$

After substituting the expressions of  $\dot{\alpha}$  e  $\dot{\hat{\mathbf{g}}}_\Gamma$  into Eq. (24), and after some algebraic manipulation, all the terms feature a dot product with the angular rate, that can be collected. Thus, after introducing the vector quantity

$$\boldsymbol{\Psi} = \frac{(\hat{\tau} \times \hat{\sigma}) + 2(1 - \cos \hat{\alpha}) (\hat{\mathbf{g}}_\Gamma \cdot \hat{\sigma}) \{ [\hat{\mathbf{g}}_\Gamma \times (\hat{\sigma} \times \hat{\mathbf{g}}_\Gamma)] (\hat{\mathbf{b}} \cdot \hat{\tau}) - [(\hat{\tau} \times \hat{\mathbf{g}}_\Gamma) \cdot (\hat{\sigma} \times \hat{\mathbf{g}}_\Gamma)] \hat{\mathbf{b}} \}}{\sin \hat{\alpha} [1 - (\hat{\mathbf{g}}_\Gamma \cdot \hat{\sigma})^2]} \|\boldsymbol{\varepsilon} \times \hat{\mathbf{b}}\| \quad (28)$$

the expression of  $\dot{\hat{\alpha}}$  assumes the compact structure  $\dot{\hat{\alpha}} = \boldsymbol{\Psi} \cdot \boldsymbol{\omega}$ .

## Appendix 2

In what follows, the equality  $\boldsymbol{\Psi} \cdot \hat{\mathbf{g}}_\Gamma = 1$  proposed in Section 2.3. is verified. Starting from Eq. (10), and recalling that  $\hat{\mathbf{b}} \cdot \hat{\mathbf{g}}_\Gamma = 0$  and  $[\hat{\mathbf{g}}_\Gamma \times (\hat{\sigma} \times \hat{\mathbf{g}}_\Gamma)] \cdot \hat{\mathbf{g}}_\Gamma = 0$ , it is straightforward to obtain

$$\boldsymbol{\Psi} \cdot \hat{\mathbf{g}}_\Gamma = \frac{(\hat{\tau} \times \hat{\sigma}) \cdot \hat{\mathbf{g}}_\Gamma}{\sin \hat{\alpha} [1 - (\hat{\mathbf{g}}_\Gamma \cdot \hat{\sigma})^2]} \quad (29)$$

provided  $\hat{\tau} \times \hat{\sigma} = \sin \alpha \hat{\mathbf{e}}_m$ , and  $\hat{\mathbf{e}}_m \cdot \hat{\mathbf{g}}_\Gamma = \cos \beta$  one has:

$$\boldsymbol{\Psi} \cdot \hat{\mathbf{g}}_\Gamma = \frac{\sin \alpha}{\sin \hat{\alpha}} \frac{\cos \beta}{[1 - (\hat{\mathbf{g}}_\Gamma \cdot \hat{\sigma})^2]} \quad (30)$$

Consider the spherical triangle ABC defined by unit vectors  $\hat{\sigma}$ ,  $\hat{\mathbf{g}}_\Gamma$ , and  $\hat{\mathbf{e}}_M$  depicted in Figure 5. The great circle length from  $\hat{\sigma}$  to  $\hat{\mathbf{e}}_M$  is  $\alpha/2$ , from  $\hat{\mathbf{g}}_\Gamma$  to  $\hat{\mathbf{e}}_M$  is  $\pi/2 - \beta$ , while the former angle in



- [7] Yoon, H. and Tsiotras, P. "Spacecraft line-of-sight control using a single variable-speed control moment gyro." *AIAA Journal of Guidance Control and Dynamics*, Vol. 29, No. 6, p. 1295, 2006.
- [8] Avanzini, G., de Angelis, E. L., and Giulietti, F. "Single-Axis Pointing of Underactuated Spacecraft in the Presence of Path Constraints." *Journal of Guidance, Control, and Dynamics*, Vol. 38, No. 1, pp. 143–147, 2015.